Author Query Form

Journal: JCP
Article: JCP26845

Dear Author,

During the copy-editing of your paper, the following queries arose.

Please refer to the query reference callout numbers in the page proofs and respond to each by marking the necessary comments using the PDF annotation tools.

Please remember illegible or unclear comments and corrections may delay publication.

Many thanks for your assistance.

Query Reference	Query	Remarks/Comments	Query Reviewed
Q1	Author: Please confirm that given names (blue) and surnames/family names (vermilion) have been identified correctly.		☐
Q2	Author: Please verify that the linked ORCID identifiers are correct for each author.		☐
Q3	Author: Organization division or department name is required for the affiliations 5 and 6. Please provide.		☐
Q4	Author: Please check and confirm the edits made in Affiliation 4.		☐
Q5	Author: Please check the hierarchy of the section headings.		☐
Q6	Author: Please provide the expansion of "DMEM."		☐
Q7	Author: Please provide a caption for Table 1, if necessary.		☐
Q8	Author: Figure 3 caption: Please define "GAPDH."		☐
Q9	Author: Please provide volume no and page range in reference Squillaro et al (2015).		☐

MPS	Journal	MSP No.	Dispatch: May 21, 2018	CE:
	JCP	26845	No. of Pages: 11	PE: Diane Punger

Received: 16 October 2017 | Accepted: 9 May 2018

DOI: 10.1002/jcp.26845

ORIGINAL RESEARCH ARTICLE

WILEY Journal of Cellular Physiology

Mesenchymal stromal cells from amniotic fluid are less prone to senescence compared to those obtained from bone marrow: An in vitro study

Nicola Alessio[1*] | Caterina Pipino[2*] | Domitilla Mandatori[3] | Pamela Di Tomo[3] | Angela Ferone[1] | Marco Marchiso[3] | Mariarosa A.B. Melone[4] | Gianfranco Peluso[5] | Assunta Pandolfi[2] | Umberto Galderisi[1,6]

[1]Department of Experimental Medicine, Biotechnology and Molecular Biology Section, University of Campania Luigi Vanvitelli, Naples, Italy

[2]Department of Medical, Oral and Biotechnological Sciences, G. D'Annunzio University Chieti-Pescara, Chieti, Italy

[3]Department of Medicine and Aging Sciences, G. D'Annunzio University Chieti-Pescara, Chieti, Italy

[4]Department of Medical, Surgical, Neurological, Metabolic and Aging Sciences, 2nd Division of Neurology, Center for Rare Diseases and InterUniversity Center for Research in Neurosciences, University of Campania Luigi Vanvitelli, Naples, Italy

[5]Institute of Bioscience and Bioresources, CNR, Naples, Italy

[6]Sbarro Institute for Cancer Research and Molecular Medicine, Center for Biotechnology, Temple University, Philadelphia, Pennsylvania

Correspondence
Assunta Pandolfi, Department of Medical, Oral and Biotechnological Sciences, "G. D'Annunzio" University Chieti-Pescara, Via dei Vestini, 66100 Chieti, Italy.
Email: assunta.pandolfi@unich.it
Umberto Galderisi, Department of Experimental Medicine, University of Campania "Luigi Vanvitelli," Via Luigi De Crecchio 7, 80138 Naples, Italy.
Email: umberto.galderisi@unicampania.it

Mesenchymal stromal cells (MSCs) are considered to be an excellent source in regenerative medicine. They contain several cell subtypes, including multipotent stem cells. MSCs are of particular interest as they are currently being tested using cell and gene therapies for a number of human diseases. They represent a rare population in tissues; for this reason, they require, before being transplanted, an in vitro amplification. This process may induce replicative senescence, thus affecting differentiation and proliferative capacities. Increasing evidence suggests that MSCs from fetal tissues are significantly more plastic and grow faster than MSCs from bone marrow. Here, we compare amniotic fluid mesenchymal stromal cells (AF-MSCs) and bone marrow mesenchymal stromal cells (BM-MSCs) in terms of cell proliferation, surface markers, multidifferentiation potential, senescence, and DNA repair capacity. Our study shows that AF-MSCs are less prone to senescence with respect to BM-MSCs. Moreover, both cell models activate the same repair system after DNA damage, but AF-MSCs are able to return to the basal condition more efficiently with respect to BM-MSCs. Indeed, AF-MSCs are better able to cope with genotoxic stress that may occur either during in vitro cultivation or following transplantation in patients. Our findings suggest that AF-MSCs may represent a valid alternative to BM-MSCs in regenerative medicine, and, of great relevance, the investigation of the mechanisms involved in DNA repair capacity of both AF-MSCs and BM-MSCs may pave the way to their rational use in the medical field.

KEYWORDS
amniotic fluid, bone marrow (BM), DNA repair, mesenchymal stromal cells (MSCs), senescence

Abbreviations: AF-MSCs, amniotic fluid mesenchymal stromal cells; ATM, ataxia telangiectasia mutated; BM-MSCs, bone marrow mesenchymal stromal cells; CFU, colony forming units; CKIs, cyclin kinase inhibitors; DNA-PK, DNA-dependent protein kinase; γ-H2AX, histone H2AX phosphorylated on Ser-140; hTERT, human telomerase reverse transcriptase.; HR, homologous recombination; Ki67, proliferation marker protein Ki67; MSCs, mesenchymal stromal cells; NHEJ, nonhomologous end joining; Oct3/4, octamer-binding transcription factor 3/4; qPCR, quantitative PCR; RAD51, DNA repair protein RAD51 homolog 1; SA-β-Gal, senescence-associated β-galactosidase; Sox-2, SRY-box 2; SSEA4, stage-specific embryonic antigen-4.

*These authors contributed equally to this work.

1 | INTRODUCTION

Mesenchymal stromal cells (MSCs), present in the stroma of bone marrow (BM) and other tissues such as fat, dental pulp, tendons, placenta, and amnios, contain a subpopulation of stem cells able to differentiate in adipocytes, chondrocytes, osteocytes, and other mesodermal derivatives. MSCs can also contribute to the homeostatic maintenance of several organs and tissues. Nonclonal MSC cultures containing a variable amount of stem cells are promising candidates for cell transplantation due to their self-renewal ability as well as their high growth rate, differentiation potential, low immunogenicity, and high anti-inflammatory properties (Galderisi & Giordano, 2014).

Nowadays, dozens of clinical trials aim to treat a number of diseases, primarily immune system-related diseases, with MSCs (Squillaro, Peluso, & Galderisi, 2015). A major concern is the large number of MSCs required for clinical trials as culture senescence affects the in vitro expansion of MSCs. This procedure is necessary to obtain an adequate number of cells for transplantation. Moreover, it has been demonstrated that the proliferation and differentiation potential of MSCs is affected by donor age (Squillaro et al., 2015).

During in vitro cultivation, human MSCs undergo telomere shortening and acquire a senescent phenotype. This can profoundly modify their regenerative and immune suppressive properties (Galipeau, 2013).

Senescence has to be considered as a dynamic process induced by genetic and epigenetic changes; it is a response to potentially oncogenic and genotoxic stimuli. These stimuli include damage to DNA, whether at telomeres or elsewhere in the genome; strong mitogenic signals, including those produced by activated oncogenes; damage or disruptions to the epigenome; and ectopic expression of certain tumor suppressors (Campisi & d'Adda di Fagagna, 2007; Capasso et al., 2015; van Deursen, 2014).

The consequences of cellular senescence are myriad. The essentially irreversible growth arrest can suppress tumorigenesis; other phenotypes of senescent cells can promote optimal tissue repair; senescent cell phenotypes can also, ironically, fuel the development of cancer; and they can cause or promote the degenerative diseases of aging (Campisi & d'Adda di Fagagna, 2007).

It would be highly desirable to expand MSCs for many passages without significant signs of senescence. In this regard, an alternative approach to BM could result from the use of MSCs derived from extraembryonic tissues such as amniotic fluid, the umbilical cord, and the placenta. Indeed, several studies have demonstrated their huge in vitro growth potential (Pipino et al., 2015).

Samples from amniotic fluid can be easily collected during amniocentesis, and MSCs can be isolated and expanded in culture for many passages from tissues that would be otherwise discarded. In addition, amniotic fluid mesenchymal stromal cells (AF-MSCs) can be easily reprogrammed in pluripotent stem cells and cryopreserved and stored at minimal cost without affecting their properties after thawing (Pipino et al., 2014). AF-MSCs have emerged as a source of stem cells with great potential in regenerative medicine that offer advantages in terms of proliferation and plasticity when compared with adult cells and allow us to avoid the ethical and safety concerns inherent in embryonic stem cells.

In this study, we compared AF-MSCs and BM mesenchymal stromal cells (BM-MSCs) in terms of growth potential and the senescence process to investigate their clinical potential use. In detail, we have examined surface markers, cell proliferation and multidifferentiation potential, senescence, and DNA repair capacity following stimulation with exogenous stressors.

2 | MATERIALS AND METHODS

2.1 | Isolation of human AF-MSCs

Human MSCs were isolated from AF-MSCs of pregnant women during routine amniocentesis at 16–18 weeks of gestation. Women received detailed information about the experimental protocol, which was approved by the Ethics Committee of the University of Chieti, and each participant gave written consent for the study. Two or 3 ml of AF was obtained from patients, and cells were immediately isolated by centrifugation at 1,200 rpm for 10 min at room temperature (RT). The supernatant was discarded, and the cell pellet was suspended in standard medium composed of low glucose Dulbecco's modified Eagle's medium (Sigma-Aldrich, Saint Louis, MO) supplemented with 15% fetal bovine serum (FBS; Gibco-Life Technologies, Monza, Italy), 5 ng/ml recombinant human basic fibroblast growth factor (bFGF; R&D Systems, Minneapolis, MN), 1% penicillin/streptomycin, and 1% L-glutamine (Sigma-Aldrich) and incubated at 37°C with 5% CO_2 in a humidified atmosphere. The first change of medium was performed after 5–7 days and nonadherent cells were removed. Then, the medium was changed every 3 days; cells were harvested when they reached 70%–80% confluence using Trypsin-EDTA and routinely subcultured at 1:3 dilution.

All experiments were performed on cells at passages 4 (P4) and/or 7 (P7) and/or 14 (P14) as specified.

2.2 | Isolation of human BMSCs

BM samples were obtained from healthy donors after written informed consent. Cells were separated on the Ficoll density gradient (GE Healthcare, Milan, Italy), and the mononuclear cell fraction was collected and washed in PBS. We seeded $1–2.5 \times 10^5$ cells/cm^2 in alpha-minimum essential medium (EuroClone, Pero, Italy) containing 10% FBS (EuroClone) and 3 ng/ml bFGF (Preprotech, London, UK). After 72 hr, nonadherent cells were discarded and adherent cells were further cultivated to confluency and amplified at P1. Then, the medium was changed every 3 days and cells were harvested when they reached 70%–80% confluence using Trypsin-EDTA (EuroClone) and routinely subcultured at 1:3 dilution. All experiments were performed on cells at P4 and/or P7 and/or P14 as specified.

2.3 | Treatment with exogenous stressors

To evaluate the potential DNA repair mechanisms of AF-MSCs and BM-MSCs, we used exogenous stressors such as doxorubicin and hydrogen peroxide (Sigma-Aldrich). In detail, both cell types at P4 were incubated

with 1 μM doxorubicin or 300 μM H_2O_2 for 30 min and analyzed after 1 hr, 6 hr, and 48 hr from the beginning of treatments.

2.4 | Flow cytometry

Briefly, cells were washed and stained for surface or intracellular antigens as previously described (Pipino et al., 2015). Surface antigens were evaluated in cells incubated with specific antibodies for 30 min at 4°C in the dark and then incubated for 5 min in 0.5% paraformaldehyde (PFA) at RT. Intracellular antigens were evaluated in fixed (Lysing solution; BD Biosciences, San Jose, CA) and permeabilized cells (Perm II; BD Biosciences). Then, cells were incubated with specific antibodies for 30 min at 4°C in the dark and for 5 min in 0.5% PFA at RT (Pipino et al., 2015).

FITC-conjugated anti-CD13, anti-CD44, anti-CD45, anti-CD105, anti-CD166, and PE-conjugated anti-CD29 were obtained from Ancell (Bayport, MN); anti-CD14-FITC was obtained from Miltenyi Biotec (Bergisch Gladbach, Germany); anti-HLA-DR-PE, anti-HLA-ABC-Alexa488, anti-CD90-FITC, anti-CD73-PE, anti-Sox-2-Alexa488, anti-SSEA-4-FITC, anti-OCT3/4-PE, anti-CD117-APC, and anti-CD146-FITC were purchased from Becton Dickinson (San Jose, CA); anti-CD144-FITC was purchased from Acris Antibodies (Herford, Germany); anti-CD34-PE was obtained from Beckman Coulter (Fullerton, CA); anti-human telomerase reverse transcriptase (hTERT) was purchased from Calbiochem (Darmastadt, Germany); and secondary FITC-conjugated was purchased from Jackson ImmunoResearch Laboratories (West Grove, PA).

2.5 | In vitro osteogenic differentiation and Alizarin Red S staining

Osteogenic differentiation was performed by culturing the AF-MSCs and BM-MSCs with DMEM medium (EuroClone) supplemented with 10% FBS (EuroClone), 0.05 mM ascorbic acid (Sigma-Aldrich), 10 mM β-glycerophosphate (Sigma-Aldrich), and 100 nM dexamethasone (Sigma-Aldrich) for 21 days, with changes of medium every 3 days. To visualize calcium sediments, cultures were stained with Alizarin Red S (Sigma-Aldrich) and the microscope images were acquired (Pipino et al., 2015).

2.6 | In vitro adipocyte differentiation and Oil Red O staining

AF-MSCs and BM-MSCs were seeded at a density of 1.5×10^4 in six-well plates and grown in standard DMEM medium (EuroClone). At 70%–80% confluence, the medium was replaced with adipogenic induction medium composed of high-glucose DMEM (EuroClone) supplemented with 10% FBS (EuroClone), 1% penicillin/streptomycin (EuroClone), 1 mM dexamethasone (Sigma-Aldrich), 10 μg/ml insulin (Sigma-Aldrich), 0.5 mM 3-isobutyl-1-methylxanthine (Sigma-Aldrich), and 200 μM indomethacin (Sigma-Aldrich). Cells were cultured in this medium for 21 days. Adipogenic differentiation was confirmed on Day 21 using an Oil Red O stain (Sigma-Aldrich) as an indicator of intracellular lipid accumulation. Briefly, cells were washed twice in PBS, fixed with 4% formaldehyde for 10 min at RT, rinsed once with 3% isopropanol, and stained with Oil Red O staining solution. Then, cells were rinsed with water and photographed under the microscope (D'Alimonte et al., 2013).

2.7 | In vitro chondrogenic differentiation and alcian blue staining

Chondrogenic differentiation was performed following an adapted protocol reported by Iacono et al. (2012). Briefly, 5×10^3 cells/cm^2 were seeded and cultured in chondrogenic medium, composed of DMEM (EuroClone), 1% FBS (EuroClone), 100 IU/ml penicillin (EuroClone), 100 mg/ml streptomycin (EuroClone), 50 nM ascorbate-2-phosphate (Sigma-Aldrich), 0.1 mM dexamethasone (Sigma-Aldrich), and 10 ng/ml human transforming growth factor-β1 (Preprotech). The medium was replaced every 3 days. To detect glycosaminoglycan formation on the cell surfaces, Alcian Blue staining (Sigma-Aldrich) was performed after 21 days as already established (Pipino et al., 2015). In short, cells were fixed in cold acetone:methanol solution for 3 min and then incubated at RT in 1% alcian blue solution for 30 min followed by three rinses in 3% acetic acid for 2 min each. After rinsing in deionized water for 2 min, the surfaces were allowed to dry for imaging.

2.8 | Colony-forming unit assay

AF-MSC or BM-MSC cultures were obtained as described above. Cultures were expanded to 70%–80% confluence. On these cells (P4), we carried out a colony-forming unit (CFU) assay as reported (Pochampally, 2008). Briefly, we plated 1,000 cells in each 10 cm culture dish and incubated them for 14 days in a growth medium. Subsequently, the medium was discarded and colonies were fixed with 100% methanol for 10 min at −20°C. Colonies were then stained with 0.01% (w/v) crystal violet (Sigma-Aldrich) in 25% methanol in PBS for 30–60 min. For every experimental condition, we counted the number of colonies in culture dishes under the light microscope.

2.9 | In situ senescence-associated β-galactosidase assay

Cells were fixed using a solution of 2% formaldehyde and 0.2% glutaraldehyde. After that, cells were washed with PBS and then incubated at 37°C for at least 2 hr with a staining solution (citric acid/phosphate buffer [pH 6], $K4Fe(CN)_6$, $K3Fe(CN)_6$, NaCl, $MgCl_2$, and X-Gal). The percentage of senescent cells was calculated by the number of blue, β-galactosidase-positive cells out of at least 500 cells in different microscope fields as already reported (Debacq-Chainiaux, Erusalimsky, Campisi, & Toussaint, 2009).

2.10 | Telomere length measurement

We used the method of Cawthon (2002). In brief, genomic DNA was extracted from cell culture samples with commercial kits. A real-time

quantitative PCR (qPCR) was performed to measure the length of telomeres. For each sample, telomeres (T) and single copy gene (S) were amplified using specific primer pairs. The T/S ratio, obtained by comparing the Ct threshold values, was used to determine the telomere relative length.

2.11 | Immunocytochemistry

Ataxia telangiectasia mutated (ATM, ab36810; ABCAM, Cambridge, UK), gamma-H2AX (2577; Cell Signaling, Denver, MA), proliferation marker protein (Ki67, sc7846; SantaCruz Biotech, Dallas, TX), DNA repair protein RAD51 homolog 1 (RAD51, ab88572; ABCAM) and DNA-dependent protein kinase (DNA-PK, sc390698; SantaCruz Biotech) were detected according to the manufacturers' protocols. Hoechst 33342 staining was performed, and then cells were observed through a fluorescence microscope (Leica Italia, Milan, Italy). The percentage of ATM-, gamma-H2AX-, Ki67-, RAD51-, and DNA-PK-positive cells was calculated by counting at least 500 cells in different microscope fields.

2.12 | Western blot analysis

Cells were lysed in a buffer containing 0.1% Triton for 30 min at 4°C. Then, 10–40 μg of each lysate was electrophoresed in a polyacrylamide gel and electroblotted onto a nitrocellulose membrane. All the primary antibodies were used according to the manufacturers' instructions. Immunoreactive signals were detected with a horseradish peroxidase-conjugated secondary antibody (SantaCruz Biotech) and reacted with ECL plus reagent (GE Healthcare). Primary antibodies used: RB1 and $p27^{KIP1}$ were from Cell Signaling; RB2/P130 were from BD Biosciences; p107 (sc-318), p53 (DOI-1), and $p21^{CIP1}$ (C-19) were from Santa Cruz Biotech; and $p16^{INK4A}$ was from ABCAM. All Abs were used according to the manufacturer's instructions.

2.13 | Statistical analysis

Statistical significance was evaluated using analysis of variance followed by Student's *t* and Bonferroni's tests. We used mixed-model variance analysis for data with continuous outcomes. All data were analyzed with a GraphPad Prism version 5.01 statistical software package (GraphPad, La Jolla, CA).

3 | RESULTS

3.1 | Characteristics of AF-MSCs and BM-MSCs

Human AF-MSCs and BM-MSCs were successfully isolated from midtrimester amniotic fluid and BM, respectively, and expanded in vitro.

Flow cytometry analysis showed that AF-MSCs and BM-MSCs expressed recognized markers of MSCs (CD13, CD29, CD44, CD73, CD90, CD105, and CD166), pericyte antigens (CD146), and stemness markers (hTERT, Oct-3/4, stage-specific embryonic antigen-4 [SSEA4], and SRY-box 2 [Sox-2]). However, they were negative for the hematopoietic markers CD14 and CD45 and the hematopoietic progenitor CD34. Also, CD117 and the surface endothelial marker CD144 were not expressed. Moreover, the absence of HLA-DR and presence of HLA-ABC suggest that these cells may be applicable in immune-mediated disorders as well as in the treatment of graft-versus-host disease (Lv, Tuan, Cheung, & Leung, 2014; Table 1).

In addition, we focus our attention on stem cell properties such as self-renewal and multipotentiality. The control of these properties is strictly linked to regulation of the stemness of MSCs. In early passages ($P \leq 3$), both cells showed strong plastic adhesion with a spindle-shaped appearance (Figure 1a,b). To investigate the differentiation capacity, both AF-MSCs and BM-MSCs were cultured in osteogenic, adipogenic, and chondrogenic differentiating media. Osteogenesis was defined by changes in cell morphology with formation of cellular aggregates and production of mineral matrix, revealed by Alizarin Red S (Figure 1c,d). Adipogenesis was determined by staining cytoplasm lipid droplets with Oil Red O (Figure 1e,f), whereas the increase in proteoglycans in chondro-differentiated cells was revealed by alcian blue staining (Figure 1g,h). We carried out a CFU assay on these cells to test their clonogenicity, that is, their ability to expand at a single-cell level, which is an important feature of self-renewing stem cells (Figure 1i,j). Altogether, these results suggest that both cell types, displaying a typical mesenchymal stem cell phenotype, showed trilineage (osteo, adipo, and chondro) differentiation and were able to form colonies.

TABLE 1

	Phenotype	
Antigens	AF-MSCs	BM-MSCs
CD13	+	+
CD14	–	–
CD29	++	+
CD34	–	–
CD44	++	++
CD45	–	–
CD73	+	++
CD90	+	++
CD105	+/–	+
CD117	–	–
CD144	–	–
CD146	+	++
CD166	+	+
HLA-ABC	+	+
HLA-DR	–	–
OCT3/4	+/–	+
SSEA-4	+	+
Sox-2	++	++
h-TERT	+/++	+/++

Note. – not detected; +/– low expression; + intermediate expression; ++ high expression. AF–MSCs, amniotic fluid mesenchymal stromal cells; BM-MSCs, bone marrow mesenchymal stromal cells.

COLOR FIG

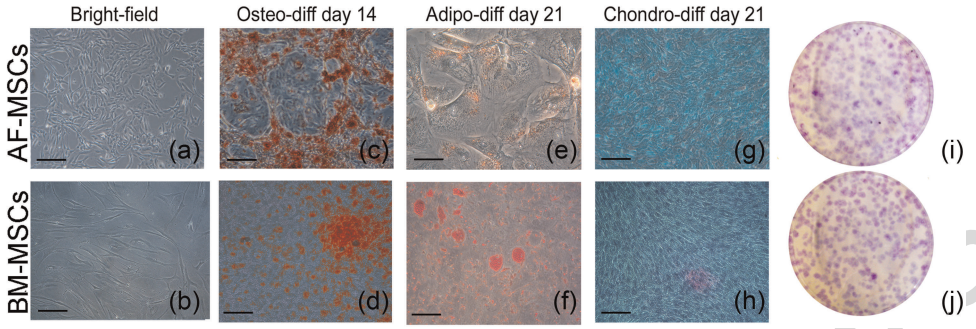

FIGURE 1 Biological features of AF-MSCs and BM-MSCs. (a,b) Bright field images of AF-MSCs and BM-MSCs before colorimetric assays cultured in standard medium. (c,d) Microscope images of Alizarin Red S staining performed 14 days after incubation in osteogenic medium. (e,f) Microscope images of both AF-MSCs and BM-MSCs cultured with adipogenic medium for 21 days evaluated by Oil Red O staining. (g,h) Representative microscopic images obtained of differentiated cells after Alcian Blue staining of cells cultivated in chondrogenic medium for 21 days. (i,j) The crystal violet staining of clones obtained is shown after 14 days of incubation at P3 of AF-MSCs and BM-MSCs. The black bars equal 100 μm. AF-MSCs, amniotic fluid mesenchymal stromal cells; BM-MSCs, bone marrow mesenchymal stromal cells

3.2 | Appearance of senescent phenotype

To follow up the appearance of senescence, the cultures were assayed for senescence-associated β-galactosidase (SA-β-Gal) activity at P4, P7, and P14 (Figure 2a). As shown in Figure 2b, the percentage of SA-β-Gal positive cells was 2.4 ± 0.3% at P4, increased to 5.3 ± 0.7% at P7, and reached 9.0 ± 1.1% at P14 in AF-MSCs; differently, BM-MSCs showed a high level of senescence already at P4 compared with AF-MSCs (8.3 ± 1.1% vs 2.4 ± 0.3%), and this difference percentage remained high up to P14 (32.5 ± 4.2% vs 9.0 ± 1.1%).

These data indicate that the proportion of senescent cells increased gradually during subcultivation of both AF-MSCs and BM-MSCs, but AF-MSCs showed later senescence compared with BM-MSCs.

These data are in agreement with the telomere length that we analysed by qPCR. In several experiments, we observed that the length of telomeres decreases progressively in BM-MSCs as amply demonstrated in the literature (Reaper, Fagagna, & Jackson, 2004), whereas it remains unchanged in AF-MSCs (Figure 2c).

The cellular response mechanism to telomere shortening is similar to the common cellular response to DNA double-strand breaks; both mechanisms go through the ATR-dependent H2AX phosphorylation. The histone H2AX phosphorylated on Ser-140 (γ-H2AX) nuclear foci indicates the presence of unrepaired or misrepaired DNA. In BM-MSCs, we observed an increase of γ-H2AX foci during in vitro expansion (Figure 2d,e), whereas in AF-MSCs, we did not observe any significant difference between passages (Figure 2d,e).

3.3 | RB and p53 cross-talk during in vitro senescence

The biological processes described are closely related to proteins that regulate cell cycle, senescence, apoptosis, and differentiation such as the RB family genes (*RB1*, *RB2*, and *P107*) and *P53* (Campisi & d'Adda di Fagagna, 2007; Helmbold, Galderisi, & Bohn, 2012).

We detected no significant change in the RB1 protein expression level during the in vitro cultivation of both AF-MSCs and BM-MSCs (Figure 3). The same trend was also observed for P107. In contrast, the RB2 expression was upregulated at P7 and P14 with respect to P4 in both cell types (Figure 3). In detail, we detected an increase in the active hypophosphorylated form. The same trend was observed for the cyclin kinase inhibitors (CKIs) $P27^{KIP1}$ and $P16^{INK4A}$. These CKIs have overlapping pathways with the RB family and P53. In particular, $p16^{INK4A}$ is often expressed in senescent cells (Campisi & d'Adda di Fagagna, 2007). During in vitro cultivation, we observed a progressive increase of $p16^{INK4A}$ and $p27^{KIP1}$ levels at P7 compared with P4, with no other changes in later phases of senescence (P14) in both MSCs (Figure 3). Both AF-MSCs and BM-MSCs showed a decrease in P53 expression during in vitro cultivation and a concomitant upregulation of MDM2, which is a P53 inhibitor (Figure 3), and downregulation of $P21^{CIP1}$, which is a major target of P53 activity (Figure 3).

3.4 | DNA damage and mechanisms of repair

The presence of persistent unrepaired or misrepaired DNA foci during in vitro cultivation prompted us to evaluate if the DNA repair mechanisms were properly activated in AF-MSCs and BM-MSCs. To better understand the differences in their repair processes, we induced DNA damage in both cell types through exogenous stressors such as doxorubicin and hydrogen peroxide. Following the induction of DNA injury, we evaluated the level of DNA damage by determining the number of damaged DNA foci per cell (γ-H2AX). As expected, H_2O_2 and doxorubicin treatment induced an increase in the number of H2AX-foci at 1 hr and 6 hr in both AF-MSCs and BM-MSCs (Figure 4). Of note, the number of H2AX-foci resulted lower in AF-MSCs versus BM-MSCs, thus displaying a better repair mechanism of AF-MSCs with respect to BM-MSCs (Figure 4). The existence of persistent unrepaired DNA

COLOR FIG

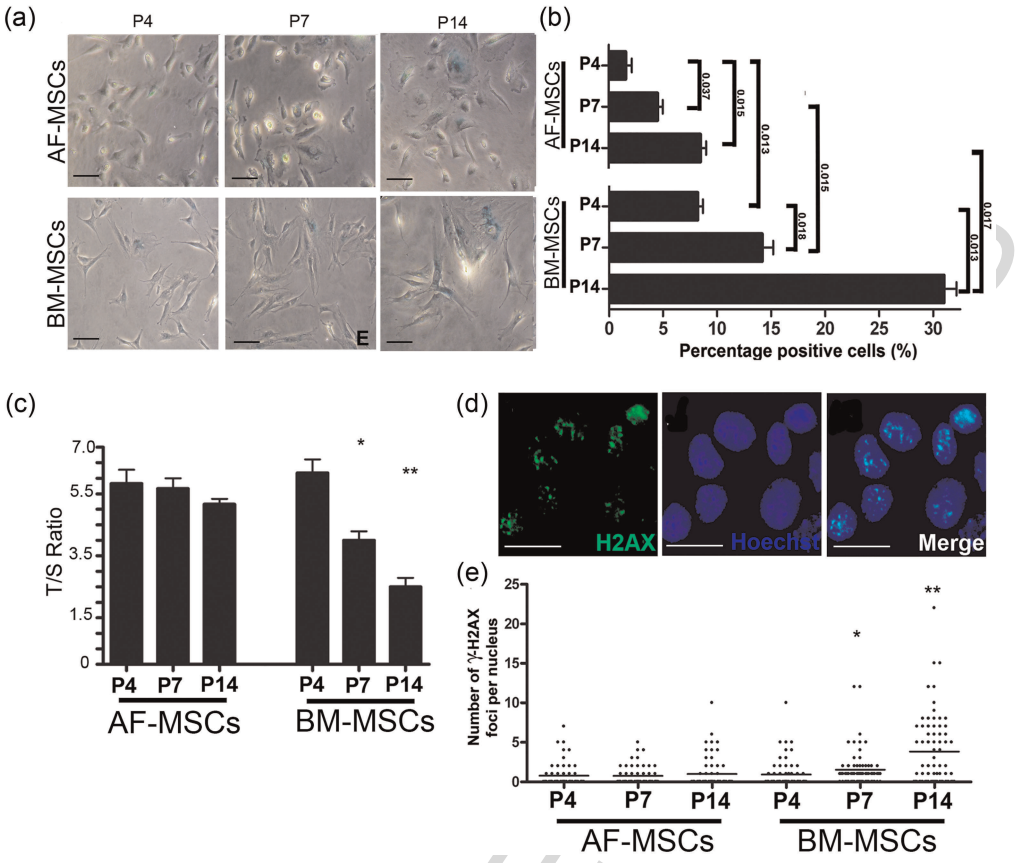

FIGURE 2 Senescence and DNA damage (a) Representative microscopic fields of acid beta-galactosidase (blue) at P4, P7, and P14 in AF-MSCs and BM-MSCs. The graph in (b) shows the mean percentage value of senescent cells (±standard deviation, $n = 3$) and P values as indicated in the figure. For each experimental condition, the relative telomere length, as determined by the T/S ratio, is shown in (c) ($n = 3$, $^{*}P < 0.05$, $^{**}P < 0.01$). The black bars equal 100 μm. (d) Representative fluorescence photomicrographs of BM-MSCs stained with anti-H2AX, Hoechst 33342, and merged. The graph in (e) shows the degree of H2AX phosphorylation in both AF-MSCs and BM-MSCs. This was evaluated by counting the number of gamma-H2AX immunofluorescent foci per cell. Foci number was determined for 200 cells. Each dot represents an individual cell. Black bars indicate the mean value for each category ($n = 3$, $^{*}P < 0.05$, $^{**}P < 0.01$). AF-MSCs, amniotic fluid mesenchymal stromal cells; BM-MSCs, bone marrow mesenchymal stromal cells

foci, as we observed for BM-MSCs, may be the trigger of senescence phenomena, as already evidenced by Campisi's team, who showed that persistent foci of damaged DNA, termed DNA-SCARS, sustain damage-induced senescence growth arrest (Rodier & Campisi, 2011).

Afterward, we determined the phosphorylation level of ATM kinase, which is a kinase that regulates DNA repair. Typically, ATM is quickly activated after DNA damage occurs (Lee & Paull, 2007). We also evaluated the expression of RAD51 and DNA-PK, downstream effectors of ATM and key regulators of homologous recombination (HR) and nonhomologous end joining (NHEJ), respectively (Kakarougkas et al., 2013; Polo & Jackson, 2011).

It is known that proteins involved in DNA repair act in pulses. Following their binding to DNA damage foci, they dissociate from the damage foci on repairing DNA (Freeman & Monteiro, 2010).

For this reason, we analyzed the expression level of proteins involved in DNA repair at 1 hr, 6 hr, and 48 hr after genotoxic stress. Our investigation was performed in cycling (Ki67+) and noncycling cells (Ki67−; Jansen et al., 1998).

Interestingly, we observed upregulation of all proteins involved in DNA repair as ATM, RAD51, DNA-PK (Figure 5).

The expression profile of ATM in cycling and noncycling cells indicates that the DNA repair system is activated soon after DNA damage and then declines to the basal level 48 hr after stress in both AF-MSCs and BM-MSCs (Figure 5a). The same trend was observed for DNA-PK and RAD51 (Figure 5b,c). The difference between AF-MSCs and BM-MSCs is in the number of cells that activated the mechanism's repair; indeed, the number of cells of AF-MSCs is major with respect to BM-MSCs. It should be noted that, following DNA damage, RAD51 expression (marker of HR) was higher in AF-MSCs than BM-MSCs. This is in agreement with a higher percentage of cells in the S-phase detected in AF-MSCs compared with BM-MSCs (Supporting Information Figure 1).

4 | DISCUSSION

MSCs have been the shining star in cell-based therapy in recent years; being characterized by unique paracrine and immunosuppressive

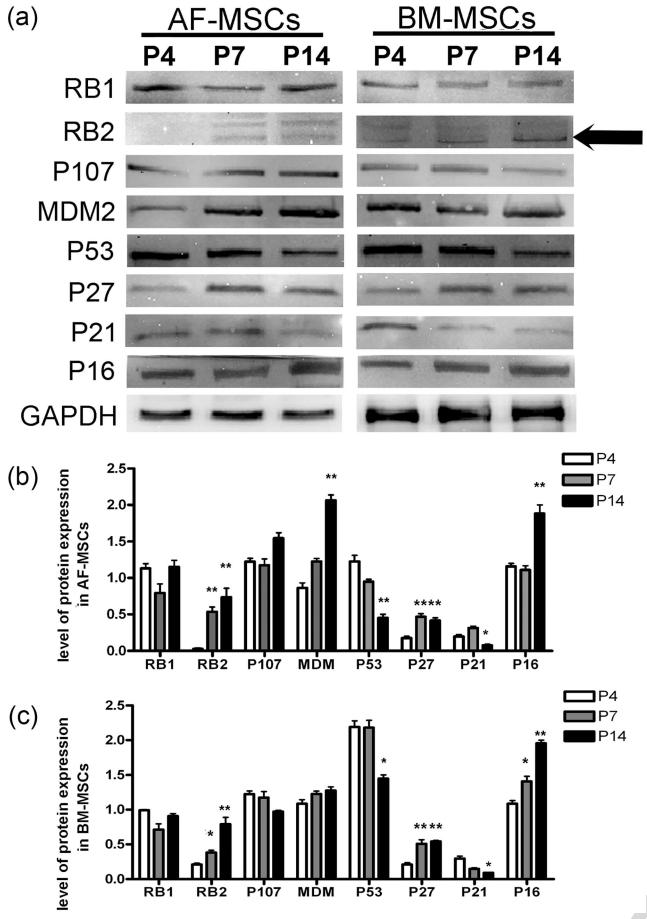

FIGURE 3 Molecular pathways involved in senescence and cell cycle arrest. (a) Western blot analysis of proteins detected in AF-MSCs and BM-MSCs at different passages in vitro. Protein levels were normalized with GAPDH as the loading control. The bar graph represents quantification of bands from independent experiments ($n = 3$, $^{*}P < 0.05$; $^{**}P < 0.01$). The arrow indicates the RB2/P130 hypophosphorylated form. AF-MSCs, amniotic fluid mesenchymal stromal cells; BM-MSCs, bone marrow mesenchymal stromal cells; GAPDH, XXX

properties makes them ideal candidates for the treatment of various diseases, including GVHD, Crohn's disease, diabetes mellitus, multiple sclerosis, myocardial infarction, liver failure, and rejection after liver transplant (Galderisi & Giordano, 2014; Squillaro et al., 2015).

Most of the application and clinical trials involve human MSCs from bone marrow (BM-MSCs; Galderisi & Giordano, 2014). Transplantation of human BM-MSCs is considered safe, and many papers with encouraging results have shown the use of these cells in clinical trials of cardiovascular, neurological, and immunological disease (Squillaro et al., 2015). However, MSCs represent a rare population in tissues; for this reason, they require, before being transplanted, an in vitro amplification.

It is well known that continued cell culture passaging induces replicative senescence, which has been linked to telomere attrition and genomic instability. Senescence can also be caused by various cell stresses, including DNA damage and oncogenes. Senescent cells can be identified by their flat and large morphology, increased SA-β-gal activity, and expression of DNA damage markers, including γ-H2AX.

Although BM has been the main source for the isolation of MSCs, recent studies have shown that MSCs could also be isolated from other tissues, including amniotic fluid, adipose tissue, endometrium, dental tissues, umbilical cord, placenta, and Wharton's jelly (Galderisi & Giordano, 2014; Pipino et al., 2014, 2013). Human AF-MSCs possess indefinite self-renewal potential, have long telomeres, and retain a normal karyotype for over 250 population doublings (Loukogeorgakis & De Coppi, 2017). Moreover, they are easy to isolate and have a high proliferation rate, thus representing a highly promising cell source for stem cell-based therapies (Shaw, David, & De Coppi, 2011).

In our study, we first compared AF-MSCs to BM-MSCs in terms of phenotype and multipotent differentiation potential. AF-MSCs had immunophenotypic characteristics similar to those of BM-MSCs with expression of CD29, CD44, CD73, CD90, CD146, and no expression of CD14, CD45, CD117, and CD144. Both cell types showed expression of the stemness markers Oct-3/4, SSEA4, Sox-2, and hTERT. The presence of HLA-ABC and the absence of HLA-DR suggest that both cell types may be suitable in the application of immune-mediated disorders.

Moreover, both cell populations were able to differentiate into mesenchymal lineages and showed self-renewal ability as demonstrated by the CFU assay. Interestingly, in our study, we demonstrated that AF-MSCs are less prone to senescence with respect to BM-MSCs when they are kept in culture for long periods (P14). We did not observe any changes in morphology of AF-MSCs until P14, whereas BM-MSCs showed slower growth and changes in morphology already at P7. These results are in accordance with reduced β-galactosidase positive cells in AF-MSCs; at P14 the β-gal positive AF-MSCs were 9.0 ± 1.1%, and the same percentage was found in BM-MSCs already at P4. Also, in agreement with Poloni et al. (2011), the length of telomeres in AF-MSCs remained stable after many passages in culture, whereas BM-MSCs showed short telomeres at P7 and even more at P14. Telomere shortening, which occurs during cell replication, is one of the factors that contribute to senescence-associated DNA damage in humans. Telomeres that are critically short become functionally "uncapped" and exhibit DNA damage with consequent phosphorylation of γ-H2AX (Nakamura et al., 2008; Takai, Smogorzewska, & de Lange, 2003).

The γ-H2AX foci are markers of damaged DNA that is undergoing the repair process, and the persistence of these foci is a sign of unrepaired DNA in cell nuclei. Our data show that telomere shortening is associated with an increase in γ-H2AX foci in BM-MSC, thus demonstrating in these cells the presence of unrepaired DNA.

Altogether, these findings clearly show that BM-MSCs are not able to be cultured longer without losing their properties, whereas AF-MSCs can be cultivated for long periods without significant alteration in their biological features.

It has been demonstrated that many types of senescence are associated with the epigenetic derepression of the cyclin-dependent kinase inhibitor 2A (*CDKN2A*) locus encoding the cell cycle inhibitor

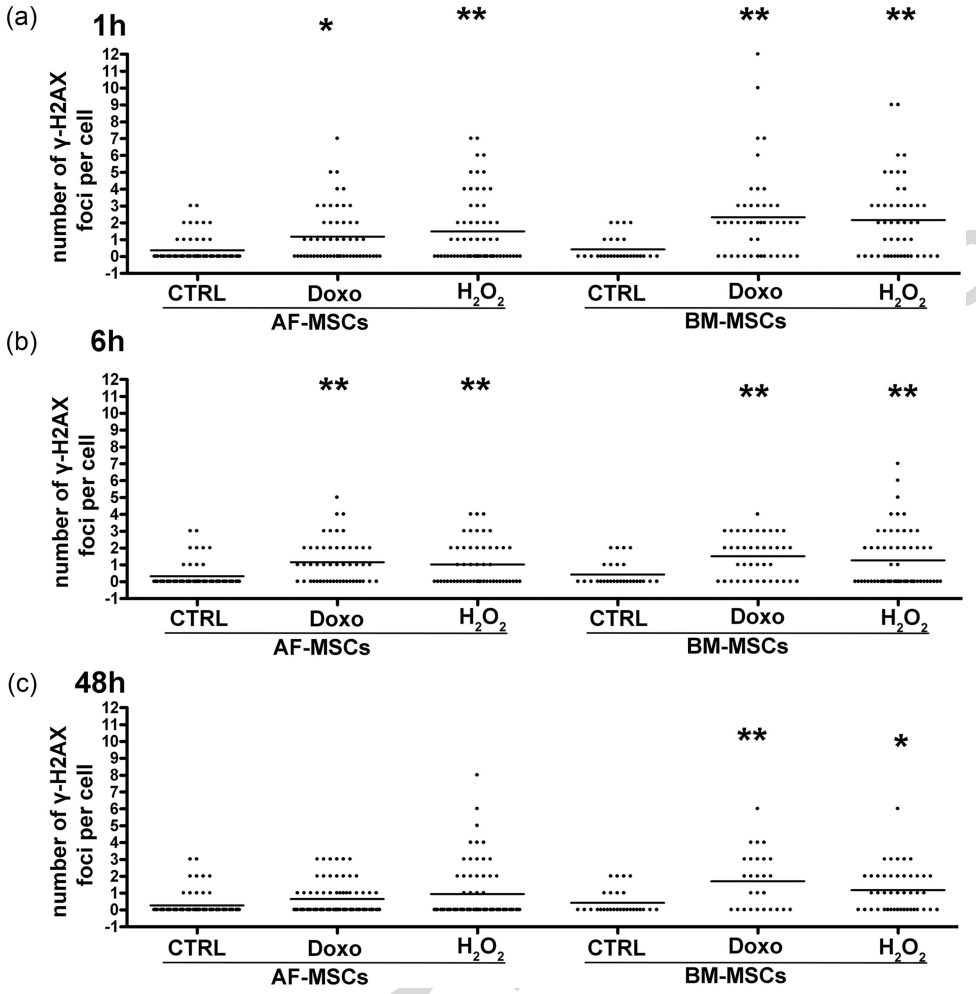

FIGURE 4 Identification of unrepaired DNA foci. The graph shows the degree of H2AX phosphorylation in AF-MSCs and BM-MSCs at three different times: 1 hr (a), 6 hr (b), and 48 hr (c) after treatment (H_2O_2 or doxorubucin) as indicated. Phosphorylation of H2AX was evaluated by counting the number of gamma-H2AX immunofluorescent foci per cell. Foci number was determined for 200 cells. Each dot represents an individual cell. Black bars indicate the mean value for each category ($n = 3$, $^*P < 0.05$, $^{**}P < 0.01$). AF-MSCs, amniotic fluid mesenchymal stromal cells; BM-MSCs, bone marrow mesenchymal stromal cells

$p16^{INK4a}$ and the p53 activator ARF (Campisi & d'Adda di Fagagna, 2007; Rodier & Campisi, 2011).

In human cells, $p16^{INK4a}$ can activate the RB1; once fully activated, the senescence cell cycle arrest becomes irreversible and is no longer revoked by subsequent inactivation of RB1, suggesting that the $p16^{INK4a}$/RB-pathway activates an alternative mechanism to irreversibly block the cell cycle in human senescent cells (Campisi & d'Adda di Fagagna, 2007; Rodier & Campisi, 2011).

For these reasons, studies on senescence mechanisms in stem cells are of great interest to dissect the pathways that may control both aberrant cell proliferation and aging phenomena.

In this study, we have investigated whether senescence was associated with RB1 or P53 pathways in both AF-MSCs and BM-MSCs. The senescence pathway in AF-MSCs and BM-MSCs is associated with the RB family gene, and it mainly involves the RB2 gene, another member of the RB family gene. Our data are in agreement with several studies demonstrating that senescence is associated with upregulation of RB2 and not of RB1 in human mesenchymal stem cells (Alessio et al., 2017).

4.1 | DNA damage response

Another more pronounced change in MSC cultures during in vitro passaging is the loss of DNA repair mechanisms. Cells with damaged DNA activate the cell cycle checkpoint to repair mechanisms. If DNA damage cannot be properly repaired, damaged cells can be eliminated either by apoptosis or by senescence (Lombard et al., 2005; Roos & Kaina, 2006).

To investigate any differences between AF-MSCs and BM-MSCs in repair mechanisms, we decided to induce DNA damage in both these cells through doxorubicin and hydrogen peroxide treatment.

H_2O_2 and doxorubicin produce multiple modifications in DNA. Oxidative attack by OH radicals on the deoxyribose moiety leads to the release of free bases from DNA, generating double strand breaks

COLOR FIG

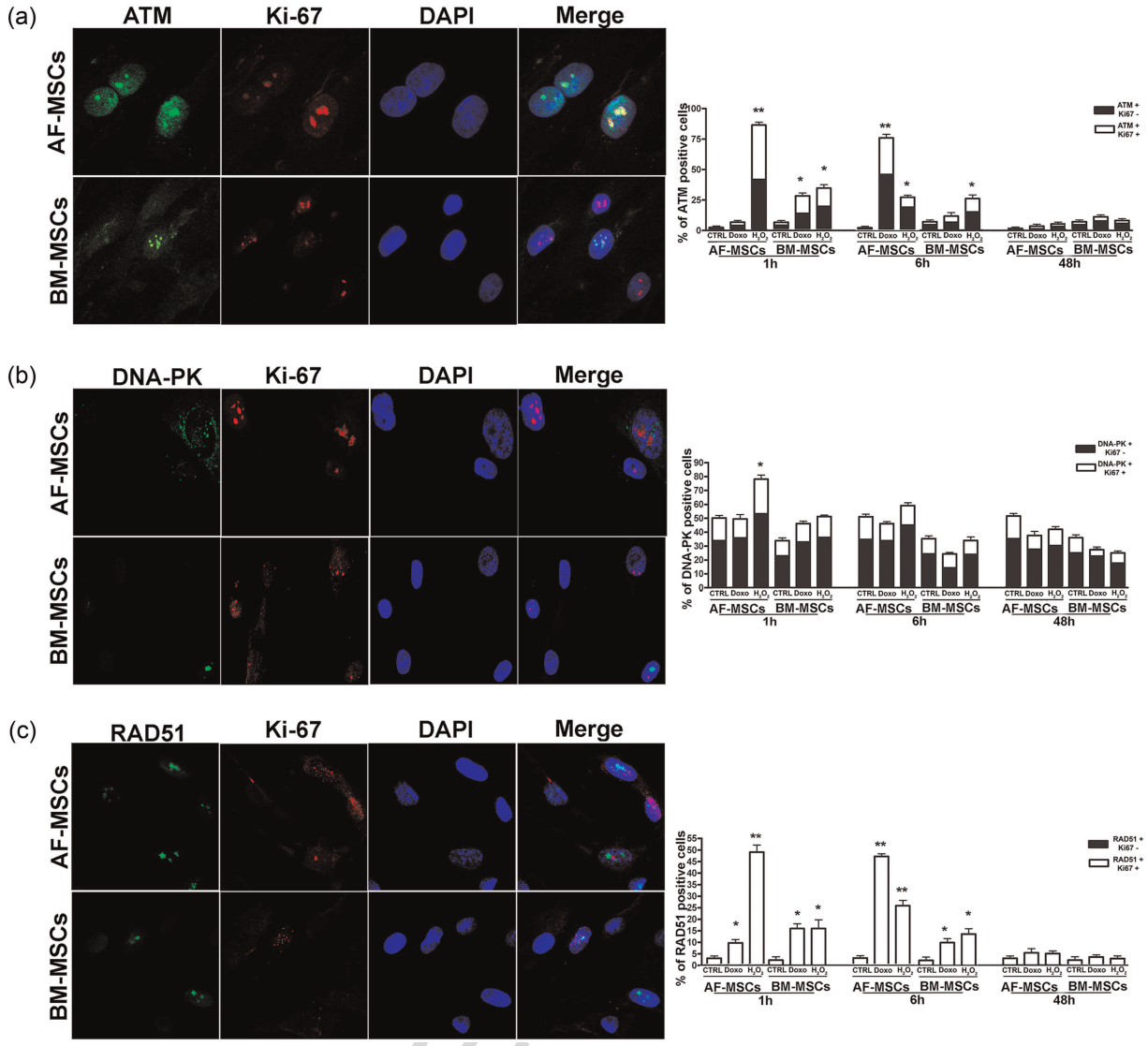

FIGURE 5 Follow-up of DNA repair after genotoxic stress. The graphs show the mean percentage of ATM (a), DNA-PK (b), and RAD51 (c) in AF-MSCs and BM-MSCs at three different times (1 hr, 6 hr, and 48 hr) after treatment (H_2O_2 or doxorubucin) as indicated, in Ki67(+) cycling cells (white bar) and Ki67(–) resting cell (black bar) (±standard deviation, $n = 3$, $^*P < 0.05$). For each detected protein, representative images of immunostaining are shown. Anti-ATM or anti-DNA-PK or anti-RAD51 showed green staining and Ki67 red staining. Nuclei were counterstained with Hoechst 33342 (blue). AF-MSCs, amniotic fluid mesenchymal stromal cells; ATM, ataxia telangiectasia mutated; BM-MSCs, bone marrow mesenchymal stromal cells; DNA-PK, DNA-dependent protein kinase; proliferation marker protein; RAD51, DNA repair protein RAD51 homolog 1

with various sugar modifications and simple abasic (AP) site (Cooke, Evans, Dizdaroglu, & Lunec, 2003).

One of the first events following DNA damage is the induction of ATM autophosphorylation (Freeman & Monteiro, 2010). This kinase triggers a complex cascade of processes leading to DNA repair, which is then dephosphorylated, and the activity of the repair system returns to basal levels.

The increase in ATM staining at 1 hr and 6 hr after treatment and its drop to basal levels at 48 hr suggest that both AF-MSCs and BM-MSCs properly activated the DNA repair signaling system. In detail, AF-MSCs activated massively the DNA repair as demonstrated by the high level of ATM, which translated into a better efficiency of the shelter to DNA as shown by the lower phosphorylated level of H2AX in AF-MSCs with respect to BM-MSCs 48 hr after treatment.

The existence of persistent unrepaired DNA foci in BM-MSCs, as evidenced by H2AX positive 48 hr after DNA damage, may be the trigger of senescence phenomena. This finding is in agreement with Campisi and collaborators, who showed that persistent foci of damaged DNA, termed DNA-SCARS, sustain damage-induced senescence growth arrest (Rodier et al., 2011).

Two prominent pathways, HR and NHEJ, mediate the repair of DNA damage in mammalian cells (Polo & Jackson, 2011; Shibata et al., 2011). HR mediates DSB repair by using a homologous stretch of DNA to guide repair of the broken DNA strand. As the name

indicates, NHEJ mediates the direct religation of the broken DNA molecule. Because NHEJ does not require a homologous template, it is not restricted to a particular phase of the cell cycle (Polo & Jackson, 2011; Shibata et al., 2011).

Therefore, we decided to investigate the repair mechanisms by analyzing each of the key proteins involved: RAD51, which has a key role in the activation of HR, and DNA-PK for NHEJ (Polo & Jackson, 2011; Shibata et al., 2011).

We observed the same trend of ATM for RAD51 and DNA-PK, thus demonstrating the same mechanism of repair in AF-MSCs and BM-MSCs.

Taken together, our results show considerable advantages of AF-MSCs compared with BM-MSCs, thus encouraging the potential application of AF-MSCs in cell therapy and regenerative medicine.

5 | CONCLUSIONS

Our study shows that AF-MSCs are less prone to senescence with respect to BM-MSCs. Both cell models are subject to the replicative senescence phenomenon but in various degrees. Indeed, AF-MSCs retain low levels of β-galactosidase even at P14 with respect to BM-MSCs.

Following DNA damage, both cell models activated the same repair system, but AF-MSCs reached basal conditions more efficiently with respect to BM-MSCs.

Although the regulatory mechanisms involved in DNA repair that we analyzed need further investigations, our study significantly supports the application of AF-MSCs in cell-based regenerative medicine.

ORCID

Mariarosa A.B. Melone http://orcid.org/0000-0002-7213-9277
Umberto Galderisi http://orcid.org/0000-0003-0909-7403

REFERENCES

Alessio, N., Capasso, S., Ferone, A., Di Bernardo, G., Cipollaro, M., Casale, F., … Galderisi, U. (2017). Misidentified human gene functions with mouse models: The case of the retinoblastoma gene family in senescence. *Neoplasia*, *19*(10), 781–790.

Campisi, J., & d'Adda di Fagagna, F. (2007). Cellular senescence: When bad things happen to good cells. *Nature Reviews Molecular Cell Biology*, *8*(9), 729–740.

Capasso, S., Alessio, N., Squillaro, T., Di Bernardo, G., Melone, M. A., Cipollaro, M., … Galderisi, U. (2015). Changes in autophagy, proteasome activity and metabolism to determine a specific signature for acute and chronic senescent mesenchymal stromal cells. *Oncotarget*, *6*(37), 39457–39468.

Cawthon, R. M. (2002). Telomere measurement by quantitative PCR. *Nucleic Acids Research*, *30*(10), e47.

Cooke, M. S., Evans, M. D., Dizdaroglu, M., & Lunec, J. (2003). Oxidative DNA damage: Mechanisms, mutation, and disease. *FASEB Journal*, *17*(10), 1195–1214.

D'alimonte, I., Lannutti, A., Pipino, C., Di Tomo, P., Pierdomenico, L., Cianci, E., … Ciccarelli, R. (2013). Wnt signaling behaves as a "master regulator" in the osteogenic and adipogenic commitment of human amniotic fluid mesenchymal stem cells. *Stem Cell Reviews*, *9*(5), 642–654.

Debacq-Chainiaux, F., Erusalimsky, J. D., Campisi, J., & Toussaint, O. (2009). Protocols to detect senescence-associated beta-galactosidase (SA-betagal) activity, a biomarker of senescent cells in culture and in vivo. *Nature Protocols*, *4*(12), 1798–1806.

Freeman, A. K., & Monteiro, A. N. (2010). Phosphatases in the cellular response to DNA damage. *Cell Communication and Signaling*, *8*, 27.

Galderisi, U., & Giordano, A. (2014). The gap between the physiological and therapeutic roles of mesenchymal stem cells. *Medicinal Research Reviews*, *34*(5), 1100–1126.

Galipeau, J. (2013). The mesenchymal stromal cells dilemma–does a negative phase III trial of random donor mesenchymal stromal cells in steroid-resistant graft-versus-host disease represent a death knell or a bump in the road? *Cytotherapy*, *15*(1), 2–8.

Helmbold, H., Galderisi, U., & Bohn, W. (2012). The switch from pRb/p105 to Rb2/p130 in DNA damage and cellular senescence. *Journal of Cellular Physiology*, *227*(2), 508–513.

Iacono, E., Brunori, L., Pirrone, A., Pagliaro, P. P., Ricci, F., Tazzari, P. L., & Merlo, B. (2012). Isolation, characterization and differentiation of mesenchymal stem cells from amniotic fluid, umbilical cord blood and Wharton's jelly in the horse. *Reproduction*, *143*(4), 455–468.

Jansen, R., Hupperets, P., Arends, J., Joosten-Achjanie, S., Volovics, A., Schouten, H., & Hillen, H. (1998). MIB-1 labelling index is an independent prognostic marker in primary breast cancer. *British Journal of Cancer*, *78*(4), 460–465.

Kakarougkas, A., Ismail, A., Klement, K., Goodarzi, A. A., Conrad, S., Freire, R., … Jeggo, P. A. (2013). Opposing roles for 53BP1 during homologous recombination. *Nucleic Acids Research*, *41*(21), 9719–9731.

Lee, J. H., & Paull, T. T. (2007). Activation and regulation of ATM kinase activity in response to DNA double-strand breaks. *Oncogene*, *26*(56), 7741–7748.

Lombard, D. B., Chua, K. F., Mostoslavsky, R., Franco, S., Gostissa, M., & Alt, F. W. (2005). DNA repair, genome stability, and aging. *Cell*, *120*(4), 497–512.

Loukogeorgakis, S. P., & de Coppi, P. (2017). Concise review: Amniotic fluid stem cells: The known, the unknown, and potential regenerative medicine applications. *Stem Cells*, *35*(7), 1663–1673.

Lv, F. J., Tuan, R. S., Cheung, K. M. C., & Leung, V. Y. L. (2014). Concise review: The surface markers and identity of human mesenchymal stem cells. *Stem Cells*, *32*(6), 1408–1419.

Nakamura, A. J., Chiang, Y. J., Hathcock, K. S., Horikawa, I., Sedelnikova, O. A., Hodes, R. J., & Bonner, W. M. (2008). Both telomeric and non-telomeric DNA damage are determinants of mammalian cellular senescence. *Epigenetics & Chromatin*, *1*(1), 6.

Pipino, C., Mukherjee, S., David, A. L., Blundell, M. P., Shaw, S. W., Sung, P., … De Coppi, P. (2014). Trisomy 21 mid-trimester amniotic fluid induced pluripotent stem cells maintain genetic signatures during reprogramming: Implications for disease modeling and cryobanking. *Cellular Reprogramming*, *16*(5), 331–344.

Pipino, C., Pierdomenico, L., Di Tomo, P., Di Giuseppe, F., Cianci, E., D'Alimonte, I., … Pandolfi, A. (2015). Molecular and phenotypic characterization of human amniotic fluid-derived cells: A morphological and proteomic approach. *Stem Cells and Development*, *24*(12), 1415–1428.

Pipino, C., Shangaris, P., Resca, E., Zia, S., Deprest, J., Sebire, N. J., … De Coppi, P. (2013). Placenta as a reservoir of stem cells: An underutilized resource? *British Medical Bulletin*, *105*, 43–68.

Pochampally, R. (2008). Colony forming unit assays for MSCs. *Methods in Molecular Biology*, *449*, 83–91.

Polo, S. E., & Jackson, S. P. (2011). Dynamics of DNA damage response proteins at DNA breaks: A focus on protein modifications. *Genes and Development*, *25*(5), 409–433.

Poloni, A., Maurizi, G., Babini, L., Serrani, F., Berardinelli, E., Mancini, S., … Leoni, P. (2011). Human mesenchymal stem cells from chorionic villi and amniotic fluid are not susceptible to transformation after extensive in vitro expansion. *Cell Transplantation*, *20*(5), 643–654.

Reaper, P. M., Fagagna, F. A., & Jackson, S. P. (2004). Activation of the DNA damage response by telomere attrition: A passage to cellular senescence. *Cell Cycle*, *3*(5), 543–546.

Rodier, F., & Campisi, J. (2011). Four faces of cellular senescence. *Journal of Cell Biology*, *192*(4), 547–556.

Rodier, F., Munoz, D. P., Teachenor, R., Chu, V., Le, O., Bhaumik, D., … Campisi, J. (2011). DNA-SCARS: Distinct nuclear structures that sustain damage-induced senescence growth arrest and inflammatory cytokine secretion. *Journal of Cell Science*, *124*(Pt 1), 68–81.

Roos, W. P., & Kaina, B. (2006). DNA damage-induced cell death by apoptosis. *Trends in Molecular Medicine*, *12*(9), 440–450.

Shaw, S. W. S., David, A. L., & De Coppi, P. (2011). Clinical applications of prenatal and postnatal therapy using stem cells retrieved from amniotic fluid. *Current Opinion in Obstetrics and Gynecology*, *23*(2), 109–116.

Shibata, A., Conrad, S., Birraux, J., Geuting, V., Barton, O., Ismail, A., … Jeggo, P. A. (2011). Factors determining DNA double-strand break repair pathway choice in G2 phase. *The EMBO Journal*, *30*(6), 1079–1092.

Squillaro, T., Peluso, G., & Galderisi, U. (2015). Clinical trials with mesenchymal stem cells: An update. *Cell Transplantation*.

Takai, H., Smogorzewska, A., & de Lange, T. (2003). DNA damage foci at dysfunctional telomeres. *Current Biology*, *13*(17), 1549–1556.

van Deursen, J. M. (2014). The role of senescent cells in ageing. *Nature*, *509*(7501), 439–446.

SUPPORTING INFORMATION

Additional supporting information may be found online in the Supporting Information section at the end of the article.

How to cite this article: Alessio N, Pipino C, Mandatori D, et al. Mesenchymal stromal cells from amniotic fluid are less prone to senescence compared to those obtained from bone marrow: An in vitro study. *J Cell Physiol*. 2018;1–11. https://doi.org/10.1002/jcp.26845

Graphical Abstract

The contents of this page will be used as part of the graphical abstract of html only. It will not be published as part of main.

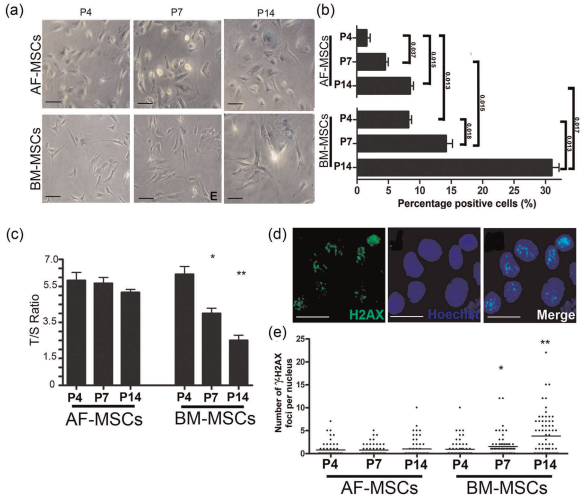

We compare amniotic fluid mesenchymal stromal cells (AF-MSCs) and bone marrow mesenchymal stromal cells (BM-MSCs) in terms of cell proliferation, surface markers, multidifferentiation potential, senescence, and DNA repair capacity. Our findings suggest that AF-MSCs may represent a valid alternative to BM-MSCs in regenerative medicine.